Electronic Supplementary Material (ESI) for Environmental Science: Water Research & Technology.

Computational framework for evaluating risk trade-offs in Legionnaires' Disease risk, energy cost, and scalding risk for hot water systems

Supplemental Information

Contents

Section 1. Implementation of heat transfer equations in the water heater

The flow of water within the water heater was modeled using a multi-node approach from Kleinbach et al., 1993 that follows **equation 1.1**.

$$\frac{dT_i}{dt} = \alpha_i \frac{v_{main}(T_{main}-T_i)}{V_i} + \beta_i \frac{v_{rec}(T_{rec}-T_i)}{V_i} + \delta_{a,i} \frac{(T_{i-1}-T_i)}{V_i} + \delta_{b,i} \frac{(T_i-T_{i+1})}{V_i} + \varepsilon Q_i - (1-\varepsilon)UA_i \qquad (1.1)$$

α_i is equal to one at the location of the mainline and zero elsewhere, β_i is equal to one at the location of the recirculating line and zero elsewhere, $\delta_{a,i}$ is equal to one when a node exists above the node of interest, $\delta_{b,i}$ is equal to one when a node exists below the node of interest, Q_i is the energy input to the system from the heating elements, UA_i is the heat lost through the heating elements when the heating elements are off. ε is a binary term that is one when the heating elements are on and zero when the heating elements are off. v_{main} is the flow rate of water entering the water heater from the main line [L/s], v_{rec} is the flow rate of water entering the uppermost node from the recirculating water line [L/s], and V_i is the volume of node i (i=1-12) [L]. T_{main} is the temperature of the municipal water from the main line [ºC], T_{rec} is the temperature of the water entering the water heater from the recirculating line [ºC], and T_i is the temperature of each node [ºC].

The final term of equation one shown in Kleinbach et al., 1993, that is not shown here is $UA_i(T_i - T_{env})$, which accounts for the heat lost to the environment through the walls of the water heater. For this model, it is assumed that the walls of the water heater are perfectly insulated and no significant heat is transferred. Therefore, the term $UA_i(T_i - T_{env})$ will go to zero and is not considered in this model. Kleinbach et al. also contains a binary γ_i term, which toggles on and off based on the quantity of water entering from the main line and the recirculating pipe. It is assumed that γ_i remains positive throughout this model so there is no reverse in the flow direction.

To use this equation, it needed to be modified into a form that was suitable for PyTorch. The α_i, β_i, $\delta_{a,i}$, and $\delta_{b,i}$ terms are all representative of their associated parameters in the water heater, but a variable ζ_i, needed to be added to account for the water exiting the heater at the hot water line, because that value will not always be equal to the volume of water entering the water heater from the recirculating line. ζ_i is equal to one at the location of the hot water line outlet and is zero everywhere else. $V_{new,i}$ accounts for the volume of water in the node at timestep t that will remain in that node at t=t+1 and is calculated by **equation 1.2**. The difference in the volume of the node V_i and $V_{new,i}$ will be the volume of water that is now in an adjacent node or the hot water line. The volume that is no longer in the node of interest will now be replaced by water from an adjacent node or the hot water line which is accounted for in **equation 1.3**.

$$V_{new,i} = V_i - \alpha_i v_{main} - \beta_i v_{rec} - \delta_{a,i} v_{mix} - \delta_{b,i}(v_{mix} + v_{main}) - \zeta_i v_{out} \quad (1.2)$$

$$T_i(t) = \frac{1}{V_i}\alpha_i v_{main} T_{main} + \beta_i v_{rec} T_{rec}(t-1) + \delta_{a,i} v_{mix} T_{i+1}(t-1) + \delta_{b,i}(v_{mix}+v_{main}) T_{i-1}(t-1) + V_{new} T_i(t-1) \quad (1.3)$$

The heat being added or lost through the heating element is considered in **equations 1.4** and **1.5**. There are two 5500 W heaters in the 316 L water heater with a 295 L storage rating (2). The two heating elements are estimated to be at nodes 3 and 9. The location of these nodes is displayed in **Figure 2** in the main manuscript. The heat entering or exiting the system can be converted from W to [ºC]/s for each node and is done so in **equations 1.4** and **1.5**.

$$Q_i = (5500\ W)\left(\frac{\frac{1.89\ CHU}{1\ hr}}{1\ W}\right)\left(\frac{1\ hr}{3600\ s}\right)\left(\frac{1\ lb\ 1℃}{1\ CHU}\right)\left(\frac{1}{57.86\ lb}\right) = 0.05℃/s\ in\ node\ i \quad (1.4)$$

$$UA_i = (550\ W)\left(\frac{\frac{1.89\ CHU}{1\ hr}}{1\ W}\right)\left(\frac{1\ hr}{3600\ s}\right)\left(\frac{1\ lb\ 1℃}{1\ CHU}\right)\left(\frac{1}{57.86\ lb}\right) = 0.005℃/s\ in\ node\ i \quad (1.5)$$

The results are added to the final temperature for nodes 3 and 9, $T_{i=3,9}(t)$ in **equation 1.6**.

$$T_{i=3,9}(t) = \begin{cases} T_{i=3,9} + Q_{i=3,9}\,t & if\ on \\ T_{i=3,9} - UA_{i=3,9}\,t & if\ off \end{cases} \quad (1.6)$$

One-dimensional mixing was chosen to be sufficient for the objective of evaluating an optimal temperature for a heterogeneous system and the multi-node model proposed allows for system parameters to be easily changed and evaluated without the use of more computationally complex computational fluid dynamics (CFD) approaches.

The chlorine (Chl_i) and planktonic *L. pneumophila* concentration (L_i) throughout the system can be calculated synchronously with the temperature by using analogous methods as shown in **equations 1.7** and **1.8**. Chl_i is the free chlorine concentration in each node i [mg/ L], and Chl_{rec} is the free chlorine concentration of the water in the recirculating line [mg/ L]. Chl_{main} is the free chlorine concentration in the water entering the system from the main line. L_i is the *L. pneumophila* concentration in each node i [CFU/ L], and L_{rec} is the *L. pneumophila* concentration reentering the water heater from the recirculating line [CFU/ L]. L_{main} is the *L. pneumophila* concentration in the water in the main line [CFU/ L].

$$Chl_i(t) = \frac{1}{V_i}\alpha_i v_{main} Chl_{main} + \beta_i v_{rec} Chl_{rec}(t-1) + \delta_{a,i} v_{mix} Chl_{i+1}(t-1) + \delta_{b,i}(v_{mix}+v_{main}) Chl_{i-1}(t-1) + V_{new} Chl_i(t-1) \quad (1.7)$$

$$L_i(t) = \frac{1}{V_i}\alpha_i v_{main} L_{main} + \beta_i v_{rec} L_{rec}(t-1) + \delta_{a,i} v_{mix} L_{i+1}(t-1) + \delta_{b,i}(v_{mix}+v_{main}) L_{i-1}(t-1) + V_{new} L_i(t-1) \quad (1.8)$$

The parameters for these variables are defined in **Table S1.**

Table S1. Model parameters for a multi-node model (Case 0 of the scenario analysis)

Parameter	Symbol	Unit	Value	Distribution	Source
Water heater set point	$Setpt$	°C	48-63	Point	(2)
Pipe lengths (Case 0: see Table 5 for summary of cases)	l_X	m	Initial Pipe: 13 Branching Pipe: 3 Recirculating Pipe: 13	Point	(3)
Number of nodes in the water heater	i	-	12	Point	(1)
Volume of node in water heater	V_i	L	24.58	Point	(2)
Volume of water entering heater from recirculating line over time	v_{rec}	L/ s	0.17	Calculated	(3)
Volume of water mixing between nodes over time	v_{mix}	L/ s	0.3	Point	(1)
Temperature of water in municipal water line	T_{main}	°C	Winter: Minimum: 16.5 Maximum: 21.5 Summer: Minimum: 17 Maximum: 24	Concatenated Uniform	(4,5)
Energy input by heating element	Q_i	°C/ s	0.05	Point	(6)
Energy lost by heating element	UA_i	°C/ s	0.005	Point	(6)
Temperature surrounding pipes	T_{env}	°C	Minimum: 20 Maximum: 27	Uniform	(7,8)
Free chlorine concentration in the water entering the system from the mainline	Chl_{main}	mg/ L	Min: 0.01 Max: 4.0	Uniform	(9)
L. pneumophila concentration in the water in the mainline	L_{main}	CFU/ L	Mean:6.60 Sd: 0.80	Lognormal	(10)

Section 2. Water velocity and Reynolds number in pipes

2.1 Water velocity in pipes

The velocity of the water in the main line and the recirculating line is typically set by the installer of the recirculating line pump. The velocity is calculated to be the minimum value to reduce energy consumption based on the user's constraint of what an acceptable heat loss for

the system will be. The velocity in the branching pipe is calculated from the flow rate of the fixture at that branch. For this system, a flow rate of 13 L/ min (low efficiency) for a “conventional” showerhead is assumed from Bastow Fjord (11,12). Using the known flow rate and the size of the branching pipe, the velocity can be calculated with the following equation where D is the pipe diameter and l_x is the length of the pipe. The velocity of the water in the hot water and recirculating lines were calculated (**equation 2.1**) to be 1.5 m/s based on pipe radius, length, and flow rate. This is also the velocity used for the water in the branching pipe when the shower is on, and zero if the shower is off. It is assumed that at least two times that flow would be required as the modeled water heater is large and would likely be serving multiple taps.

$$v = \frac{flow\ rate}{\pi\left(\frac{D}{2}\right)^2 l_x} \tag{2.1}$$

There will be a multitude of factors that will determine the value of velocity flowing through the system. The physical parameters that will influence the velocity include the pipe diameter, length, bends, fittings, tap opening, and mixing valve(s). The only parameters considered to influence the velocity in this model are the pipe diameter, length, and a single shower fixture. The water pressure should also be taken into consideration, as the water pressure can vary greatly, and pressure boosters may be installed depending on the water pressure entering the premise plumbing from the city line. All these factors will also influence the velocity of water in the recirculating line. It should also be acknowledged that with a smaller branching pipe, the velocity will be greater than that in the pipe and the recirculating line. This was not addressed in the current model.

For this model, it is assumed that the velocity will be constant at all points in the pipes when the water is not stagnant in the branching pipe. In a physical system, the velocity will constantly be changing as different taps are opened, and in some systems the recirculating line will be off for a period to save energy. The recirculating line is assumed to be running for the entirety of the model.

The necessary flow rate in m/ s is determined by the tolerable amount of heat lost in the system (3.3°C) using the equation described in **SI Section 3** solved for velocity resulting in **equation 2.2.** U is the overall heat transfer coefficient [W/ m^{2}K], L is the length of the recirculating pipe [m], c_p is the specific heat of water, ρ is the density of water, D is the diameter of the pipe, T_0 is the temperature of the water entering the pipe from the water heater, T_F is T_0 minus the tolerable loss of heat in the pipe, and T_{env} is the temperature of the environment.

$$v = \frac{-4UL}{c_p \rho D\ ln\left(\frac{T_F - T_{env}}{T_0 - T_{env}}\right)} \tag{2.2}$$

2.2 Reynolds number

Reynolds number (Re) can be calculated by **equation 2.3** for the pipe ¾” in diameter (D) [m] and the ½” diameter branching pipe that leads to the showerhead. The kinematic viscosity of water, $\frac{\mu}{\rho}$ [m^2/ s], is the viscosity (μ) over the density of water (ρ) (**Table S2**). This resulted in a velocity of 3.04 m/s and a *Re* in the pipe and branch of 52,349 and 41,444, respectively. These values of the Reynolds number are consistent with turbulent flow.

$$Re = \frac{\rho v D}{\mu} \quad (2.3)$$

The parameters for these variables are defined in **Table S2.**

Table S2. Parameters for velocity and Reynolds number

Parameter	Symbol	Unit	Value	Distribution	Source
Specific heat of water	c_p	J / kgK	4186.8	Point	(13)
Density of water	ρ	kg / m^3	996	Point	(13)
Overall heat transfer coefficients	U	W / m^2K	Uninsulated: 325.9 Insulated: 29.80	Calculated	Supplemental Information, Section 2
Diameter	D	m	Pipe: 0.019 Shower: 0.012	Point	(3)
Kinematic viscosity of water **(50°C)**	$\frac{\mu}{\rho}$	m^2/ s	5.53×10^{-7}	Point	(13)

Section 3. Heat loss in pipes

The water heater in this model is assumed to be perfectly insulated and will experience no transfer of heat from the water to the environment, however heat loss is considered in the pipes (**equation 3.1**) T [ºC] is the temperature of water in the pipe, T_{env} [ºC] is the air temperature in the air surrounding the pipe, U [W/ m^2K] is the overall heat transfer coefficient specific to that pipe configuration, c_p [J/ kg K] is the specific heat of water, ρ [kg/ m^3] is the density of water, v [m/ s] is water velocity, and D [m] is the diameter of the pipe.

$$\frac{dT}{dt} = (T(t) - T_{env})\left(\frac{-4U}{c_p \rho v D}\right) \quad (3.1)$$

Section 4. Heat transfer coefficients

To track the heat lost through the pipes, the overall heat transfer coefficient U [W/ m^2K] was calculated for each pipe size and insulation.

4.1 Convective heat transfer coefficient

The convective heat transfer coefficient, h_{conv} [W/ m^2K], is the rate at which energy is transferred from the water to the copper pipes. To find h_{conv}, an energy balance equation can be performed starting with **equation 4.1**, where $\dot{E}_{in}$ is the amount of energy entering the shared water to copper surface from the water by convection ($\ddot{q}_{conv}$) and $\dot{E}_{out}$ is the energy leaving the shared water to copper surface and going into the copper pipe by conduction ($\ddot{q}_{cond}$).

$$\dot{E}_{in} - \dot{E}_{out} = 0 \quad (4.1)$$

$$\ddot{q}_{conv} - \ddot{q}_{cond} = 0 \quad (4.2)$$

The equations for convective ($\ddot{q}_{conv}$) and conductive ($\ddot{q}_{cond}$) heat flux [W/ m^2] can be described by **equations 4.3** and **4.4** respectively. T_s is the temperature at the shared surface, T_f is the temperature of the fluid, and T_i is the temperature of the conductive material. k is the thermal conductivity of the conductive material [W/ mK], and L is the radial length of the conductive material [m].

$$\ddot{q}_{conv} = h_{conv}(T_s - T_f) \tag{4.3}$$

$$\ddot{q}_{cond} = k\frac{(T_i - T_s)}{L} \tag{4.4}$$

Substituting $\ddot{q}_{conv}$ and $\ddot{q}_{cond}$ into **equation 4.2** and solving for h_{conv} results in equation 4.5.

$$h_{conv} = \frac{k(T_i - T_s)}{L(T_s - T_f)} \tag{4.5}$$

4.2 Radiative heat transfer coefficient

The radiative heat transfer coefficient from a conductive material (copper or insulation) to air (h_{rad}) [W/ m^{2}K], can be calculated by another energy balance equation with the radiative heat flux ($\ddot{q}_{rad}$) [W/ m^2].

$$\ddot{q}_{cond} - \ddot{q}_{rad} = 0 \tag{4.6}$$

The equation for radiative heat flux ($\ddot{q}_{rad}$) can be described by **equation 4.7**.

$$\ddot{q}_{rad} = h_{rad}(T_s - T_f) \tag{4.7}$$

Equation 4.7 and **equation 4.4** can be substituted into **equation 4.6** and solved for h_{rad} resulting in **equation 4.8**.

$$h_{rad} = \frac{k(T_i - T_s)}{L(T_s - T_f)} \tag{4.8}$$

4.3 System specific variables

To calculate the heat lost to the environment from the water in the pipes, the convective and radiative heat transfer coefficients were calculated. **Figure S1** describes the temperatures and radial lengths used to calculate the convective heat transfer between the water and the copper h_{conv} (**equation 4.5**), the radial heat transfer between copper and air for uninsulated pipes $h_{rad,cu}$ (**equation 4.9**), and the radial heat transfer between insulation and air $h_{rad,ins}$ (**equations 4.10**).

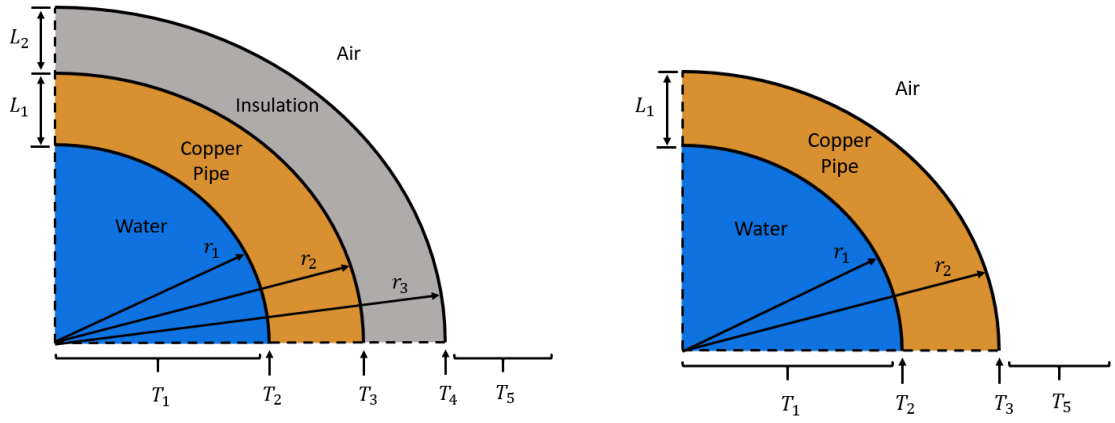

Figure S1: Cross-section of insulated pipe (left) and uninsulated pipes (right) with locations of temperatures and radial lengths.

The temperature of the fluid in the pipe was chosen as the mean of the tested temperature range (48-63 ºC) at $T_1 = 55.50℃$. The temperature of the shared water to the copper surface was set to be close to the temperature of the fluid in the pipe at $T_2 = 55.10℃$. The temperature of the shared copper to insulation surface was set to be close to the temperature of the shared water to the copper surface at $T_3 = 55.01℃$. The temperature of the outer insulation surface was set to be near the temperature of the surrounding room temperature at $T_4 = 33.5℃$. The temperature of the air surrounding the pipe was set to the average room temperature at $T_5 = 23.5℃$ (7,8). L_1 is the radial length of the copper pipe and L_2 is the radial length of the insulation [m]. k_{cu} is the thermal conductivity of commercial copper and k_{ins} is the thermal conductivity of rubber used for insulation [W/ mK].

$$h_{rad,cu} = \frac{k_{cu}(T_2 - T_3)}{L_1(T_3 - T_5)} \tag{4.9}$$

$$h_{rad,ins} = \frac{k_{ins}(T_3 - T_4)}{L_2(T_4 - T_5)} \tag{4.10}$$

The heat transfer coefficients will vary greatly based on the individual system parameters. For this model, the three heat transfer coefficients, h, were found to be within the expected values (13) for forced convection (25-250 and 100-20,000 $\left[\frac{W}{m^2K}\right]$) for gases and liquids, respectively. The parameters for these variables are defined in **Table S3.**

Table S3 Parameters for heat transfer coefficient calculation

Parameter	Symbol	Unit	Value	Distribution	Source
Thermal conductivity of commercial copper	k_{cu}	W/ mK	401	Point	(13)
Thermal conductivity of rubber (for insulation)	k_{ins}	W/ mK	0.16	Point	(13)

Radial length of copper pipe	L_1	m	0.005	Point	(3)
Radial length of insulation	L_2	m	0.013	Point	(3)
Temperature of water	T_1	℃	55.5	Point	(6)
Temperature at shared water/copper interface	T_2	℃	55.1	Point	Assumption based on (13)
Temperature at shared copper/insulation or copper/air interface	T_3	℃	55.01	Point	Estimation
Temperature at shared insulation/air interface	T_4	℃	33.5	Point	Estimation
Temperature of air surrounding pipes	T_5	℃	23.5	Point	(7,8)
Inner radius of copper pipe	r_1	m	0.009	Point	(3)
Outer radius of copper pipe/ inner radius of insulation	r_2	m	0.014	Point	(3)
Outer radius of insulation	r_3	m	0.027	Point	(3)

4.4 Overall heat transfer coefficient

The overall heat transfer coefficient for heat leaving uninsulated ($U_{uninsulated}$) and insulated ($U_{insulated}$) [W/ m^{2}K] pipes are calculated using the convective and radial heat transfer coefficients (see **Table S3** for radius definitions). The results are displayed in **Table S4.**

$$U_{uninsulated} = \left(\frac{1}{h_{conv}} + \frac{r_1}{k_{cu}}\ln\left(\frac{r_2}{r_1}\right) + \left(\frac{r_1}{r_2}\right)\frac{1}{h_{rad,cu}}\right)^{-1} \quad (4.11)$$

$$U_{insulated} = \left(\frac{1}{h_{conv}} + \frac{r_1}{k_{cu}}\ln\left(\frac{r_2}{r_1}\right) + \frac{r_1}{k_{ins}}\ln\left(\frac{r_3}{r_2}\right) + \left(\frac{r_1}{r_3}\right)\frac{1}{h_{rad,ins}}\right)^{-1} \quad (4.12)$$

The parameters for these variables are defined in **Table S4.**

Table S4: Calculated values for heat transfer coefficients and overall heat transfer coefficients

Parameter	Symbol	W/ m^{2}K
Convective heat transfer between water and copper	h_{conv}	20,050

Radial heat transfer between copper and air for uninsulated pipes	$h_{rad,cu}$	254
Radial heat transfer between insulation and air	$h_{rad,ins}$	27
Overall heat transfer coefficient (uninsulated)	$U_{uninsulated}$	315
Overall heat transfer coefficient (insulated)	$U_{insulated}$	20

Section 5. Chlorine decay

First-order decay of free chlorine is commonly calculated with a first-order decay rate (**equation 5.1**) (14,15), but it lacks any variability due to system parameters, such as temperature, total organic carbon (TOC) or differences between the bulk decay and the wall decay.

$$C = C_0 e^{-kt} \tag{5.1}$$

Instead, an Arrhenius equation was determined to be the best chlorine decay model for this system because it accounts for the influence of temperature throughout the system and parameters had already been estimated (14). The Arrhenius equation that was used is defined in **equation 5.2**. A is the pre-exponential factor, E_a is the activation energy [J/ mol], R is the universal gas constant [J/ mol K] and T is the absolute temperature [K]. This equation can be used to describe the decay of chlorine in bulk water (16).

$$k_b = A e^{\frac{-E_a}{RT}} \tag{5.2}$$

Equation 5.2 was modified by AWWARF 1996 (**equation 5.3** and **Table S5**). The pre-exponential factor is dependent on the constant a, the concentration of TOC, and the constant b, which encompasses the activation energy and the universal gas constant. T is the temperature in Kelvin. This equation allows for the free chlorine decay rate to be estimated at varying temperatures and TOC concentrations in the system.

$$k_b = a * TOC * \exp\left(\frac{-b}{T}\right) \tag{5.3}$$

However, the authors caveat this equation is not applicable beyond the range of 5°C to 25°C due to their observed experimental range. In the absence of similar data outside this range, the kinetic equation was applied for the system temperatures in the current model. The parameters for these variables are defined in **Table S5.**

Table S5 Parameters for Chlorine Decay

Parameter	Symbol	Unit	Value	Distribution	Source
Measured Constant a	a	L/ mg h	1.8×10^6	Point	(14)
Total Organic Carbon	TOC	mg/ L	Min: 1 Max: 3	Uniform	(14)

Measured Constant b	b	K	6,323	Point	(14)
Water Temperature	T	K	Measured	Point	(14)

Section 6. *L. pneumophila* growth and inactivation due to temperature

L. pneumophila has been observed multiplying in water temperatures from 25°C to 45°C (17,18) and is known to become inactivated from 50°C to 70°C (19). No growth or inactivation has been quantified in between 45°C and 50°C or below 25°C in these studies.

6.1 Inactivation rates

The inactivation rates for temperatures from 50°C to 70°C were calculated by assuming a first-order inactivation of *L. pneumophila* by **equation 6.1**.

$$C_f = C_i e^{-k_{temp} t} \tag{6.1}$$

The time for a 4-log reduction of *L. pneumophila* sg. 1 ATCC 33152 was provided in Cervero-Aragó et al., 2015. The time to reduction was found for 50°C (117 minutes), 55°C (10 minutes), 60°C (2 minutes), 65°C (0.8 minutes), and 70°C (0.9 minutes). The first-order decay equation was solved for the inactivation rate (k_{temp}) of *L. pneumophila* at different temperatures using the known 4-log reduction $\log(C_f/C_i)$, and time t (**equation 6.2**).

$$k_{temp} = \frac{-\log\left(\frac{C_f}{C_i}\right)}{t} \tag{6.2}$$

6.2 Growth rates

Sharaby et al., 2017 and Yee and Wadowsky, 1982 recorded values for *L. pneumophila* growth at 25°C, 30°C, 37°C, and 42°C. No significant growth was seen at 45°C. A first-order growth of *L. pneumophila* was assumed (**equations 6.1** and **6.2**), with a positive k_{temp} rate. Calculated first-order growth constants are shown in **Table S6**. The current model does not address the lag phase of growth described by Sharaby, 2017.The growth rates from Sharaby, 2017 were chosen to be used with the inactivation rates from Cervero-Aragó et al., 2015 for this model because it was more recent than Yee and Wadowsky, 1982. The final values k_{temp} are displayed in **equation 6.3** [s^{-1}]. The growth limit of planktonic *L. pneumophila* was set to $10^{4.17}$ CFU/ L (18). The parameters for these variables are defined in **Table S7.**

$$k_{temp} = \begin{cases} -7.41 \times 10^{-2} & if\ T_{all} \geq 70℃ \\ -8.33 \times 10^{-2} & if\ 65℃ \leq T_{all} < 70℃ \\ -3.33 \times 10^{-2} & if\ 60℃ \leq T_{all} < 65℃ \\ -6.67 \times 10^{-3} & if\ 55℃ \leq T_{all} < 60℃ \\ -5.70 \times 10^{-5} & if\ 50℃ \leq T_{all} < 55℃ \\ 0 & if\ 45℃ \leq T_{all} < 50℃ \\ 3.14 \times 10^{-5} & if\ 42℃ \leq T_{all} < 45℃ \\ 6.97 \times 10^{-5} & if\ 37℃ \leq T_{all} < 42℃ \\ 3.22 \times 10^{-5} & if\ 30℃ \leq T_{all} < 37℃ \\ 2.55 \times 10^{-5} & if\ 20℃ \leq T_{all} < 30℃ \\ 0 & if\ T_{all} < 20℃ \end{cases} \quad (6.3)$$

Table S6: Derived *L. pneumophila* growth rates

Temperature	**Growth rate per second Yee and Wadowsky, 1982**	**Growth rate per second Sharaby, 2017**
25°C	2.30×10^{-5}	2.55×10^{-5}
32/30°C	3.08×10^{-5}	3.22×10^{-5}
37°C	4.73×10^{-5}	6.97×10^{-5}
42°C	4.82×10^{-5}	3.14×10^{-5}

Table S7: Growth and inactivation rates of *L. pneumophila*

Parameter	**Symbol**	**Unit**	**Value**	**Distribution**	**Source**
Growth/inactivation Rates of *L. pneumophila* **with temperature**	k_{temp}	s^{-1}	>70°C: -7.41×10^{-2} 65-70°C: -8.33×10^{-2} 60-65°C: -3.33×10^{-2} 55-60°C: -6.66×10^{-3} 50-55°C: -5.69×10^{-5} 45-50°C: 0.0 42-45°C: 4.82×10^{-5} 37-42°C: 4.73×10^{-5} 30-37°C: 3.08×10^{-5} 20-30°C: 2.30×10^{-5}	Point	(17,19)
Planktonic *L. pneumophila* inactivation rate due to chlorine	$k_{p,chl}$	s^{-1}	Chl<0.01: 0 0.01<Chl<0.15: 1.82×10^{-3} 0.15<Chl<0.35: 1.92×10^{-3} 0.35<Chl_{all}: 2.31×10^{-2}	Point	(20)
Planktonic *L. pneumophila* growth limit		CFU/L	$10^{4.17}$	Point	(18)

Section 7. Biofilm kinetics in the pipes

The mass of biofilm per unit area (M_b [g/ cm^2]) was calculated with **equation 7.1** using the biofilm density (D_b [g/ cm^3]) (21) and the mean volume of biofilm per cm^2 of pipe area based on the biofilm thickness (V_b) [cm^3/ cm^2] (21).

$$M_b = D_b V_b \tag{7.1}$$

These values were chosen from the low turbulent flow simulation from Garny et al., 2009. This was selected as the most appropriate scenario for the current model. The data was extracted for both the biofilm density and the biofilm thickness using GetData Graph Digitizer® v2.26.0.20 software. A normal curve truncated at zero was fit to the biofilm density, D_b, for calculations and a mean value was found to be 34.5 kg/ m^3. The average thickness of the biofilm was 0.01 cm, which equates to a mean volume of biofilm per cm^2 (V_b) of 0.01 cm^3. Using these averages, the density of biofilm per cm^2 of pipe area was modeled as a normal distribution truncated at zero with an average value of 3.5×10^{-4} g/ cm^2. The biofilm sloughing rate $S_b(t_s)$ was chosen from the low turbulent flow simulation from Garny et al., 2009. The data for the biofilm sloughing rate was extracted using Digitizer software and modeled as a lognormal distribution with an upper truncation limit of 20 gDW/ m^{2}day. The average sloughing rate based on this distribution was 7.39×10^{-9} g/ cm^{2}s.

The quantity of *L. pneumophila* in the biofilm, C_b, was extracted from Figure 6.12 in (22). The mean values for the reactor were 13 CFU/ cm^2 for a heated condition and 39 CFU/ cm^2 at ambient temperature. The quantity of *L. pneumophila* for the reactor at ambient temperature was chosen and modeled as a lognormal distribution and decay rates due to temperature were applied appropriately (**SI Section 6**). The quantity of biofilm being sloughed into the water will decline as a first-order function as the shower remains on by the values in **equation 7.2** (15). It is assumed that there is no sloughing in the branch pipe when the shower is off and the water is stagnant.

$$k_s = \begin{cases} -1.30 & if\ t_s \leq 5\ min \\ -0.06 & if\ t_s > 5\ min \end{cases} \tag{7.2}$$

The quantity of sloughed *L. pneumophila* is C_s. The rate of decay of the biofilm sloughing, k_s, is modeled in **equation 7.2** using two decay rates that are dependent on how long the shower has been on (t_s) (15). The decay rate of sloughing is applied in **equation 7.4**. Based on data presented in Huang et al. (2020), we assume that *L. pneumophila* that has been sloughed from the biofilm will decay due to both chlorine in the system and the water temperature. The inactivation rates for *L. pneumophila* in the biofilm due to chlorine, $k_{b,chl}$, are presented in **equation 7.3** (15). The final *L. pneumophila* concentration in the system due to biofilm sloughing is calculated using **equation 7.4**. The amount of biofilm that is sloughed will decay in concentration due to k_s, and will experience inactivation due to the chlorine decay rate $k_{b,chl}$ times the concentration chlorine residual, Chl, as well as experiencing growth or inactivation from temperature k_{temp}. Biofilm calculation parameters are summarized in **Table S8**.

$$k_{b,chl} = \begin{cases} -0.46 & if\ t_s \leq 5\ min \\ -0.10 & if\ t_s > 5\ min \end{cases} \tag{7.3}$$

$$C_s(t) = C_{s,0}\, e^{(k_s + k_{b,chl} Chl + k_{temp}) t_s} \tag{7.4}$$

Table S8. Biofilm parameters

Parameter	Symbol	Unit	Value	Distribution	Source
Biofilm density	D_b	kg / m^3	Shape: 3.14 Scale: 38.66	Weibull*	(21)
Volume of biofilm per m^2	V_b	m^3 / m^2	1×10^{-4}	Point	(21)
Concentration of *L. pneumophila* **in biofilm**	C_b	CFU / m^2	Min: 3.9×10^5 Max: 7.8×10^9	Uniform	(22,23)
Duration of shower	t_s	s	μ: 465 σ: 72	Normal	(24)
Sloughing rate of biofilm	$S_b(t_s)$	g / cm^2s	Mean log: -18.96 Sd log: 0.709	Lognormal	(21)
Decay of sloughing rate	k_s	min^{-1}	-1.30: $t_s \leq 5$min -0.06: $t_s > 5$min	Point	(15)
Decay of sloughed *L. pneumophila* **in biofilm due to chlorine**	$k_{b,chl}$	$(mg/L*min)^{-1}$	-0.46: $t_s \leq 5$min -0.10: $t_s > 5$min	Point	(15)

*Modeled as a uniform distribution for Sobol Sensitivity Analysis

Section 8. Initialization of the system

To initialize the system:

1. The water heater system was run for 24 hours with no shower and no new water from the main line to mimic stagnation events. The temperature, chlorine, and *L. pneumophila* will act according to the equations described in **Section 2** (Methods) of the manuscript. After 24 hours, the initialized temperature throughout the system is recorded and stored for later.
2. The *L. pneumophila* growth and decay throughout the water heater, hot water line, and recirculating line needed to be estimated beyond the growth and decay rates shown in **Table S7**. While the system runs, the water temperature can pass through different temperature zones that either inactivate or promote the growth of *L. pneumophila*. This change in water temperature throughout the system will change with pipe length, water velocity, or other physical parameters. The volume of water at different temperatures will also vary depending on the location in the plumbing system. For example, a smaller amount of water will be at a cooler temperature at the end of the recirculating line than the water in node 3 or 9 of the water heater which contain sthe heating elements and has a larger volume. Therefore, to determine the *average* inactivation or growth rate of *L. pneumophila* due to temperature for the 24-hour initialization period in the water heater, hot water line, and recirculating line, a mass balance equation was performed with the

initialized temperature and volume of each section of the system. The initialized inactivation or growth rates were recorded for each case and stored for later use.

3. For each iteration of the Monte Carlo simulation, the initialized temperature and inactivation or growth rates were loaded. The temperature of the system was set as the previous initialized temperature for each case.
4. To initialize the free chlorine values for the water heater, hot water line, and recirculating line, the free chlorine concentration was calculated using the Arrhenius equation for each Monte Carlo iteration (**SI Section 5**). The time that it took the chlorine to decay to be below the limit that it would affect the *L. pneumophila* was calculated. The *L. pneumophila* concentration after the 24-hour initialization period was then calculated using the previously recorded initialized inactivation or growth rates applied over the time that the chlorine was below the limit that would affect the *L. pneumophila* growth. The *L. pneumophila* growth in the branching pipe was calculated as a first-order growth equation with the room temperature growth rate applied over 24 hours.
5. A growth cap was applied over the entire system so the *L. pneumophila* concentration did not exceed $10^{4.17}$ CFU/ L (18).
6. The biofilm was calculated for each case as described in **Section 2.7** of the main manuscript. The initialized inactivation or growth rates for *L. pneumophila* were applied to the biofilm in the hot water line and recirculating line for 24 hours. No chlorine decay was applied. The variables used to calculate the biofilm are from sources that conducted experiments at room temperature (21–23), therefore, there was no inactivation or growth rate applied to the biofilm in the branching pipe that remained at room temperature for the 24-hour initialization period.

Section 9. Decay of aerosols and QMRA parameters

The decay of aerosols d_i [s^{-1}] that have been released into the exposure environment was calculated using the aerosol removal rates, d_{1-2} [min^{-1}], from Huang et al., 2020 with the percentage of aerosol sizes, F_{1-10}, from Hamilton et al., 2019. It is a weighted average based on the difference aerosol removal rates for the two aerosol size bins of consideration: 1-2 micrometers and 3-10 micrometers. The decay of the aerosols is calculated in **equation 8.1** and displayed in **Table S9.** The parameters used for the quantitative microbial risk assessment (QMRA) are displayed in **Table S10** and described in **Section 2.8** of the main manuscript.

$$d_i = d_1 F_{1-2} + d_2 F_{3-10} \quad (8.1)$$

Table S9: Calculated aerosol decay values

Parameter	Variable	Value	Unit
Percent aerosols 1-2 micrometer	F_{1-2}	33.89	%
Percent aerosols 3-10 micrometer	F_{3-10}	66.11	%

Aerosol Removal Rate <=2 micrometer	d_1	0.35	1/min
Aerosol Removal Rate >2 micrometer	d_2	1.24	1/min
Decay of aerosols	d_i	0.016	1/s

Table S10 QMRA parameters

Parameter	Symbol	Unit	Value	Distribution	Source
Concentration of aerosols	C_{aero}	CFU/ m^3	1-2: μ: 17.5, σ: 0.30 2-3: μ: 17.5, σ: 0.17 3-6: μ: 19.4, σ: 0.35 6-10: μ: 20.0, σ: 0.31	Lognormal	(12,25)
Volume of aerosols	V_{areo}	L/ CFU	1-2: Min: 5.25×10^{-16} Max: 4.19×10^{-15} 2-3: Min: 4.19×10^{-15} Max: 1.41×10^{-14} 3-6: Min: 1.42×10^{-14} Max:1.13×10^{-13} 6-10: Min: 1.13×10^{-13} Max:5.22×10^{-13}	Uniform	(12,25)
Fraction of *L. pneumophila* that partition to each of the aerosol diameters	F	%	1-2: 0.34 2-3: 0.16 3-6: 0.13 6-10: 0.17	Point	(26)
Alveolar deposition efficiency	D	Fraction	1-2: 0.23-0.53 2-3: 0.36-0.62 3-6: 0.10-0.62 6-10: 0.01-0.29	Uniform	(Heyder et al., 1986)
Rate of inhalation	B	m^3/ min	0.013-0.017	Uniform	(28)

Decay of aerosols	d_i	s^{-1}	-0.016	Point	(11,15)
Dose response parameter for sub-clinical infection	k_s	s^{-1}	Mean: -2.93 Sd: 0.49	Lognormal	(29,30)
Dose response parameter for clinical infection	k_c	s^{-1}	Mean: -9.69 Sd: 0.30	Lognormal	(29,30)
Disability adjusted life year	$DALY$	years	0.97	Point	(31)
Value of a statistical life	VSL	USD	Min:5,324,706 Max: 17,368,683	Uniform	(32)
Remaining Life expectancy	*Life expectancy*	years	Mean: 31.88 Sd: 18.32 Min: 0	Truncated Normal	(33)
Morbidity Ratio, elderly	MR_e	Unitless	0.75	Point	(34)

Section 10. Scalding and energy costs

The cost of scalding was calculated using data from Moritz and Henriques (1947) (35). Data in the original work were presented in coordinates of temperature and time based on two categories of severity of injury: epidermal injury and epidermal necrosis. A log of the data on both axes was used so linear regressions could be calculated. The points for epidermal injury (mild-moderate injury) were used to find a linear regression shown in red below in **Figure S2**. The points for epidermal necrosis (moderate-severe injury) were used to find a linear regression shown in blue below. The 95% confidence intervals are shaded in grey around each regression.

- **Epidermal Injury:** y = -0.0342x + 1.783
- **Epidermal Necrosis**: y = -0.0359x + 1.793

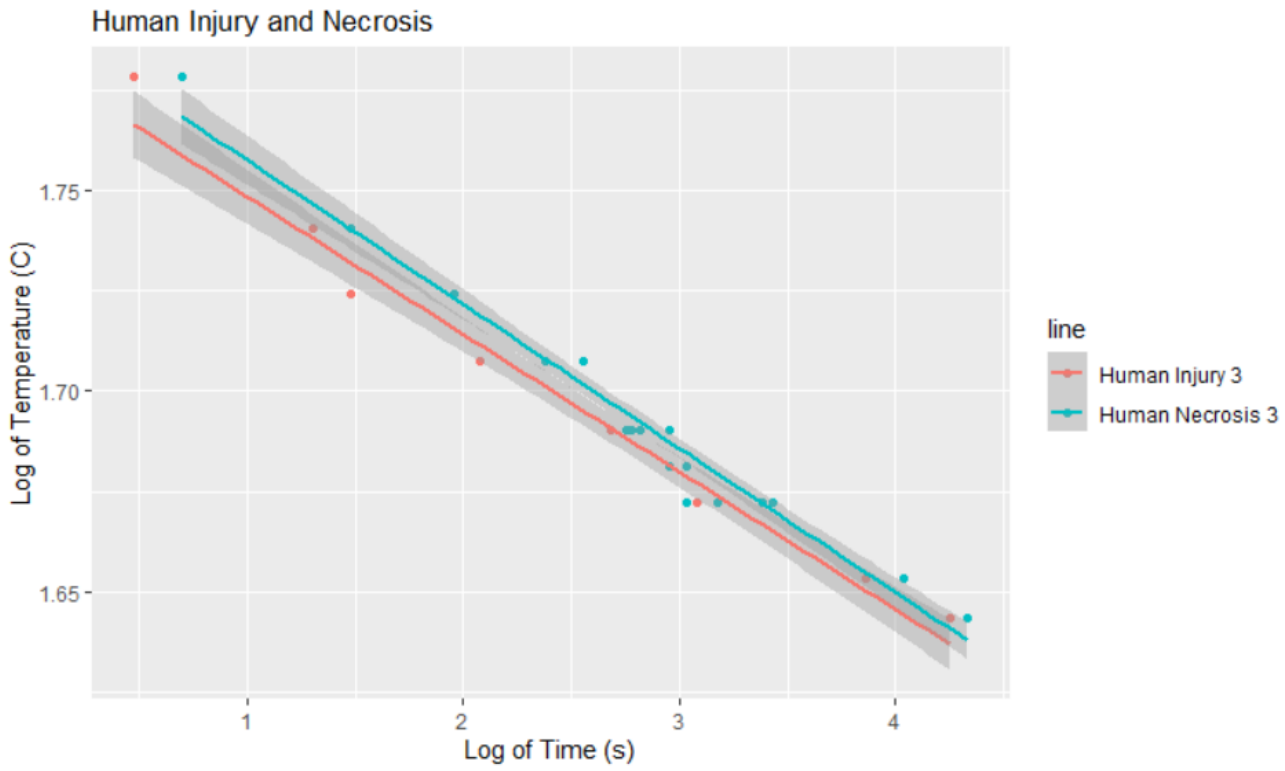

Figure S2. The scalding curve for epidermal injury (red) and epidermal necrosis (blue) based on the log of time and log of temperature.

The Monte Carlo model then determined where the severity of the injury lies for each iteration based on the temperature of the water at the showerhead and the time it took for the individual to remove themselves from the water (uniform distribution randomly sampled from 1.0 to 5.0 seconds).

Once it was determined which region each iteration was within, a monetary value was assigned based on approximate costs for each category.

- **No injury** (blue): $0.00
- **Epidermal injury** (yellow): $141.76 to $221.89 (uniform distribution randomly sampled)
- **Epidermal necrosis** (red): $628.69 to $862.90 (uniform distribution randomly sampled)

Differences in datasets could not be evaluated directly with statistical tests due to lack of alignment between temperature and time points (i.e. measurements that occurred at different times and different temperatures could not be directly compared). The regressions used were not statistically significant from each other ($p>0.05$). Once an injury has begun, if the stimulus is not removed there will only be a small amount of time until the injury progresses. We considered expanding the data set by adding the extensive dataset from pig injury and necrosis in Table 2 of Moritz and Henriques (35) which is plotted in **Figure S3**. Adding these data did not change the conclusion that the regressions associated with the two injury categories are not significantly different. Merging the human data in **Figure S2** was also considered shown in **Figure S4**, however the small region between the two regressions indicates that there is a small range of temperatures before the onset of burn where there is a physiological difference in burn outcome—a mild burn for a short duration. The merged scenario is a scenario that can be chosen by the

user in the code for this model. A sensitivity analysis for the cost of the injury or necrosis was estimated using data from Blue Cross Blue Shield, 2009, and is displayed in **Table S12**.

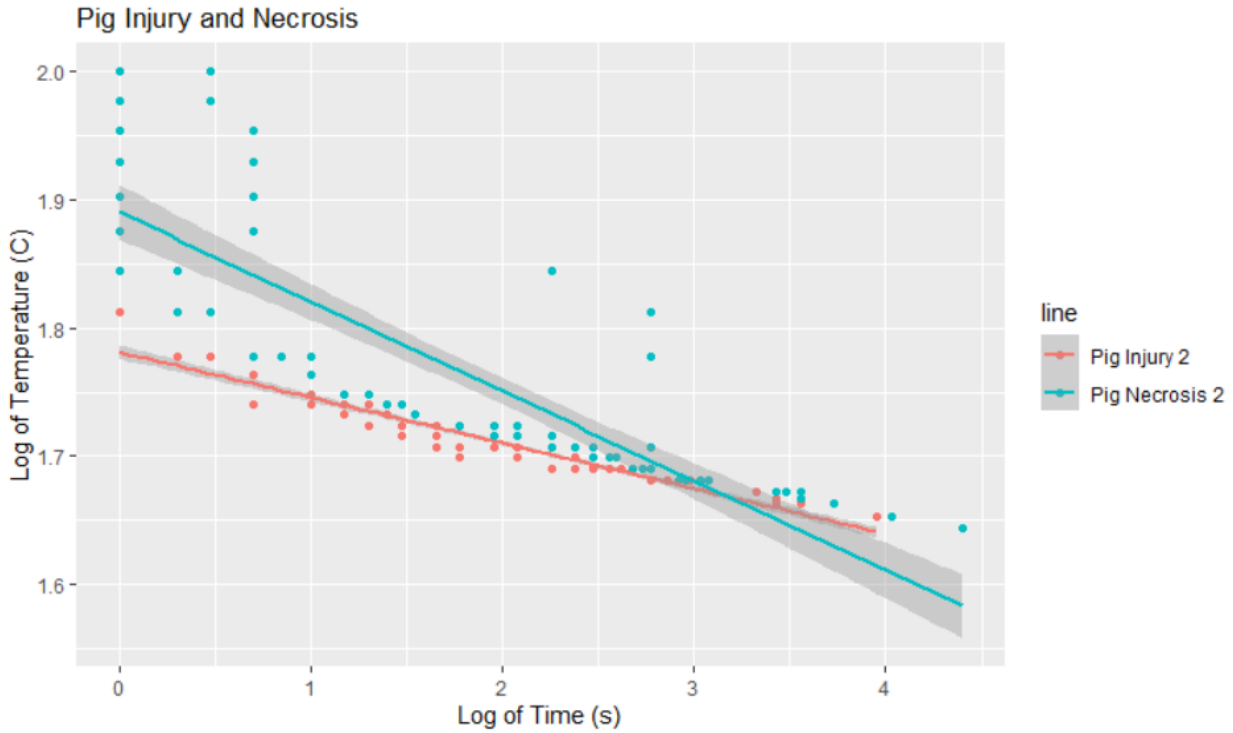

Figure S3. The scalding curve for epidermal injury (red) and epidermal necrosis (blue) based on log of time and log of temperature for pig data.

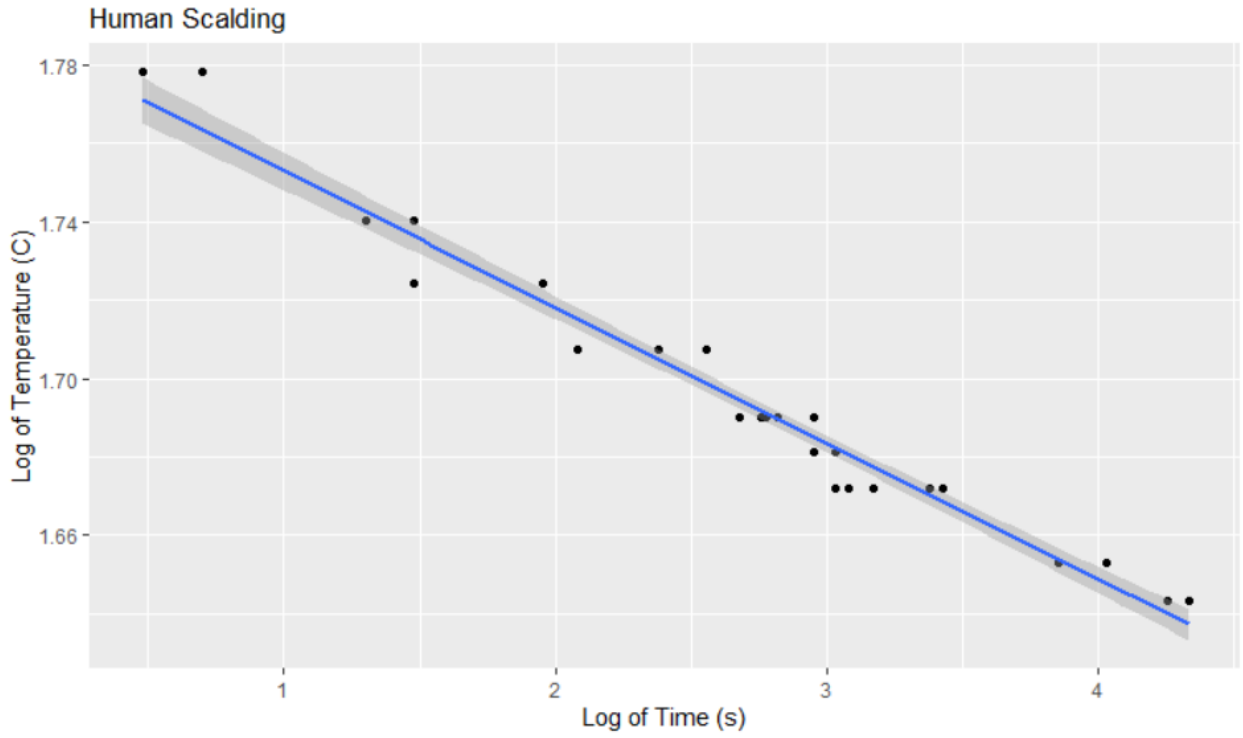

Figure S4. The scalding curve for epidermal injury and epidermal necrosis together based on log of time and log of temperature for human data. Regression equation log(y) = -0.0347*log(x) + 1.788.

Table S11: Sensitivity analysis for three-category scald vs. two-category scald

Case	Three scald categories for human data (no injury, injury, necrosis -Fig S2)	Pooled scalding data with categories for injury with human data (injury or necrosis) vs. no injury (Fig. S5)	Difference in modeled optimum water heater set point
0	55	56	+1
1	54	54	0
2	55	59	+4
3	56	59	+4
4	55	59	+4
5	59	56	-3
6	61	59	-2
7	59	56	-3
8	48	48	0
9	48	48	0
10	48	48	0
11	48	48	0
12	55	52	-3
13	48	48	0
14	55	53	-2
15	48	48	0

Table S12: Scalding model and energy model parameters

Parameter	Symbol	Unit	Value	Distribution	Source
Burn categories	$injury\ type$	USD	Focal epidermal necrosis: Min: 141.76 Max: 221.89 Complete epidermal necrosis: Min: 628.69 Max: 862.90	Uniform	(36)
Reaction time	$jumptime$	s	Min: 1 Max: 5	Uniform	Estimation
Liters of water used for showering daily	Q_{in}	L / Day	59	Point	U.S. Geological Survey

Price per kWh	P_{kWh}	USD / kWh	Mean: -2.01 Sd: 0.25	Lognormal	(37)
Energy Factor	EF	-	Min: 0.90 Max: 0.95	Uniform	(38)

Section 11. Additional results

A complete set of outputs for the risk of infection, total cost, and heatmaps of water quality parameters throughout the premise plumbing system are shown in **Figures S13-S14**, respectively.

	Case 0
48°C	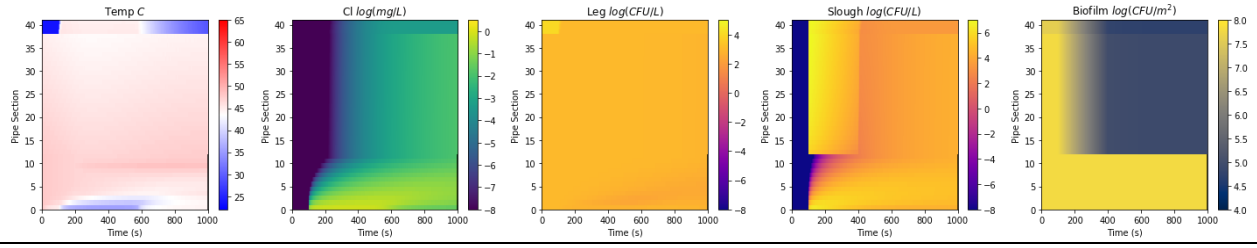
49°C	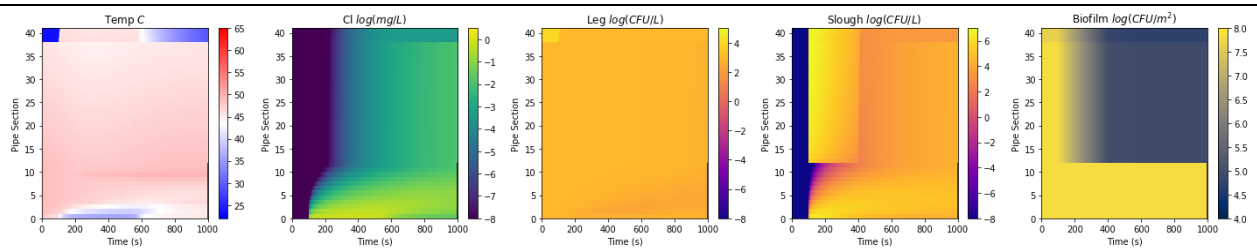
50°C	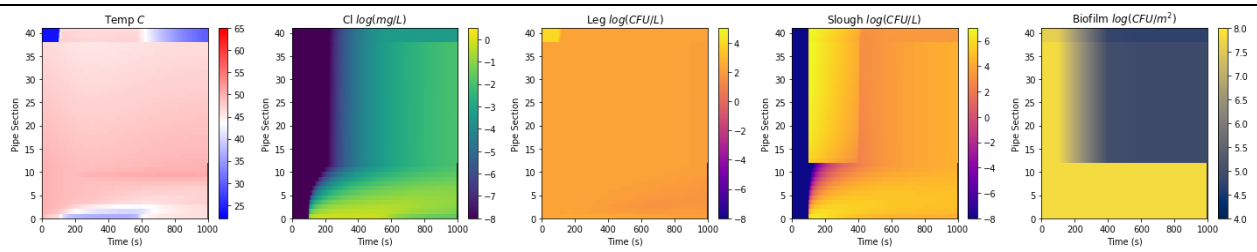
51°C	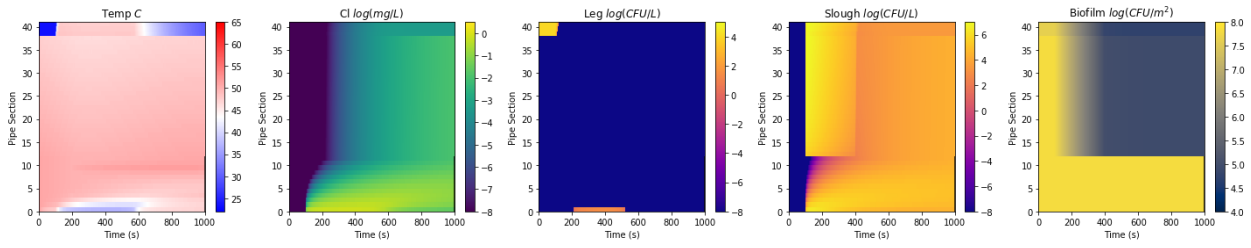

52°C	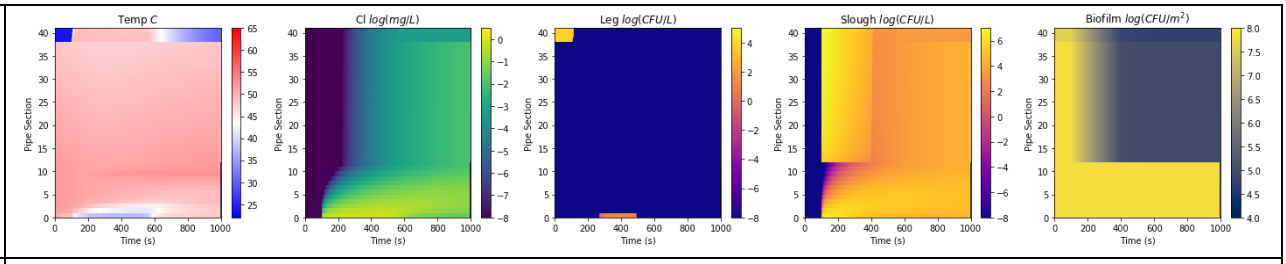
53°C	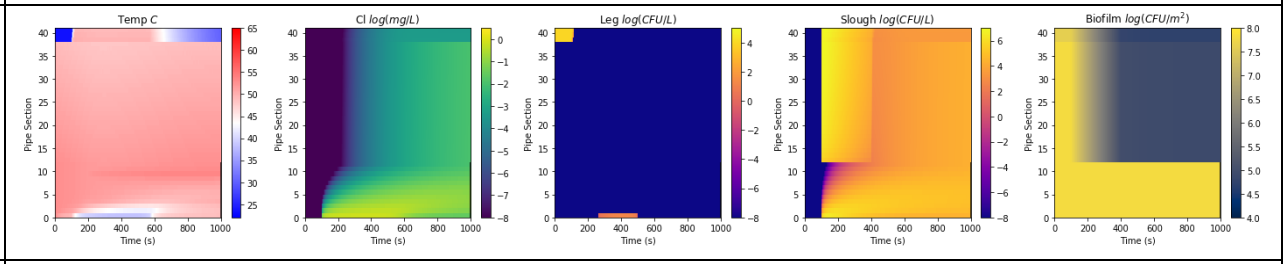
54°C	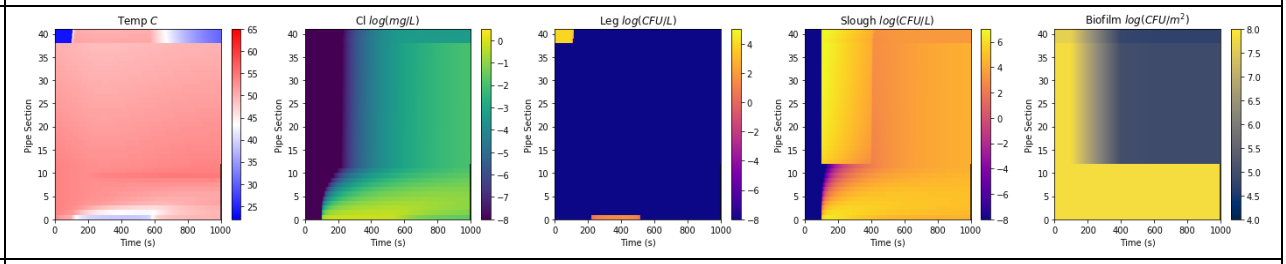
55°C	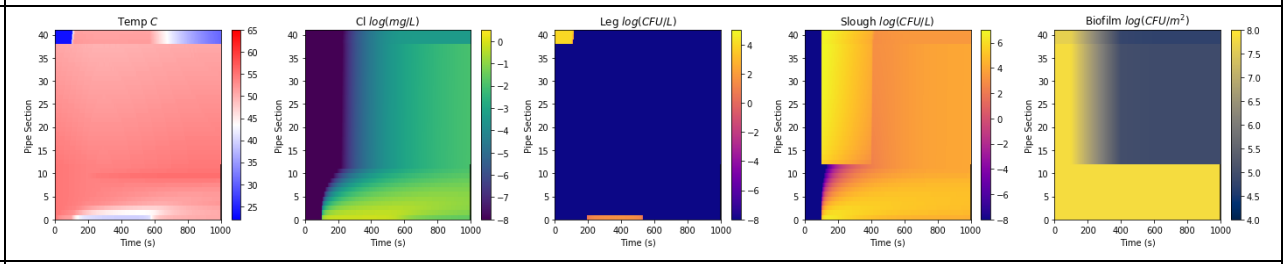
56°C	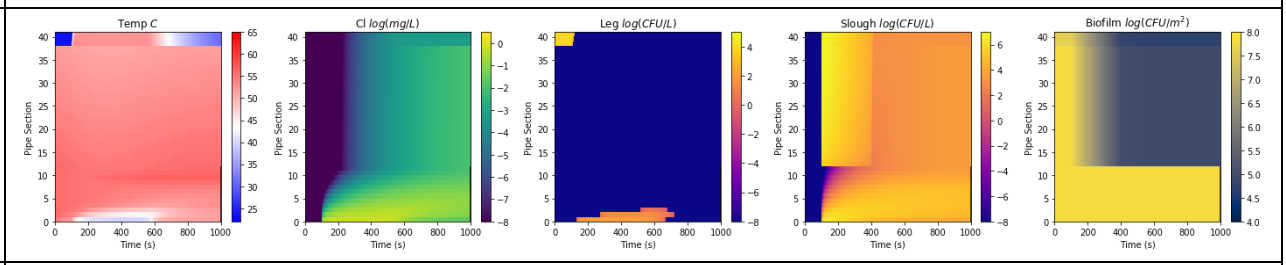
57°C	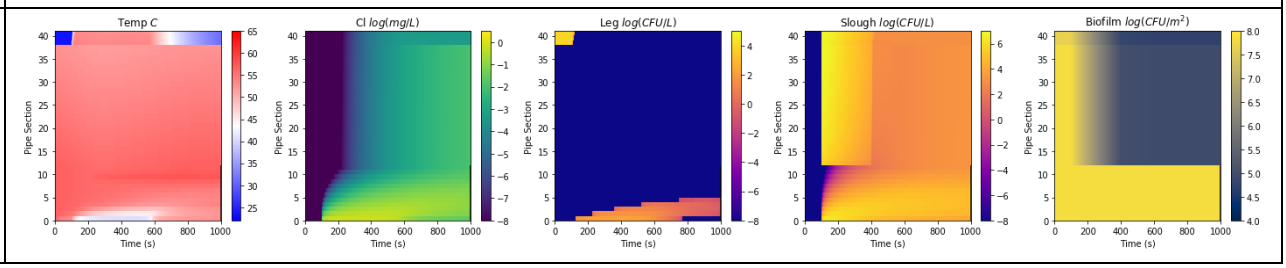

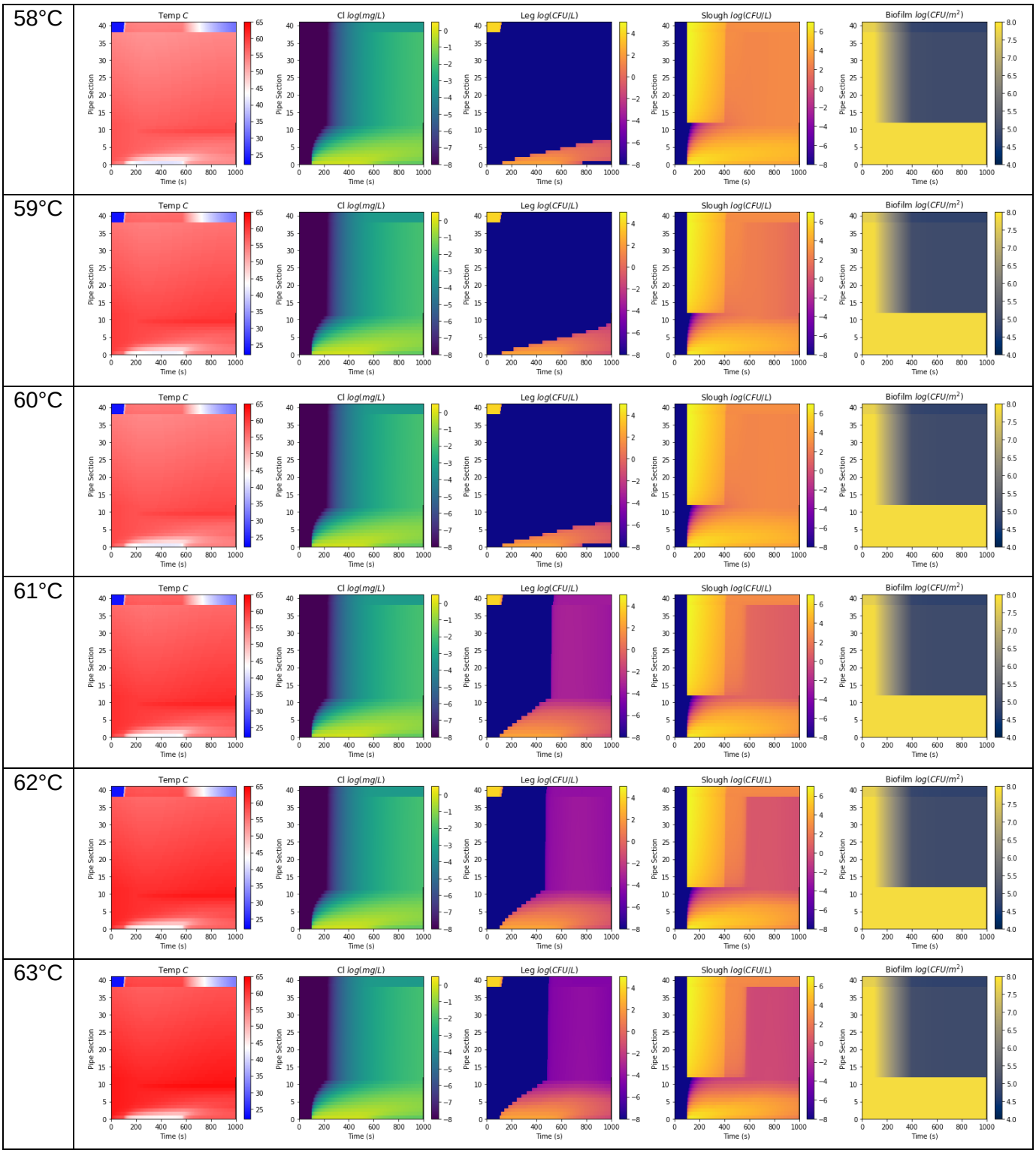

Figure S13: Heatmaps for temperature, chlorine residual, planktonic *L. pneumophila,* sloughed *L. pneumophila,* and *L. pneumophila* remaining in the biofilm.

Case	Risk of Infection or Illness	Total Cost
0	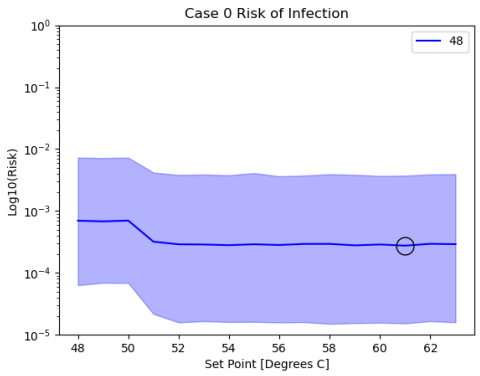	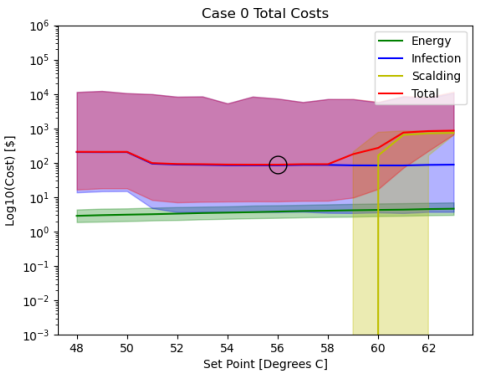
1	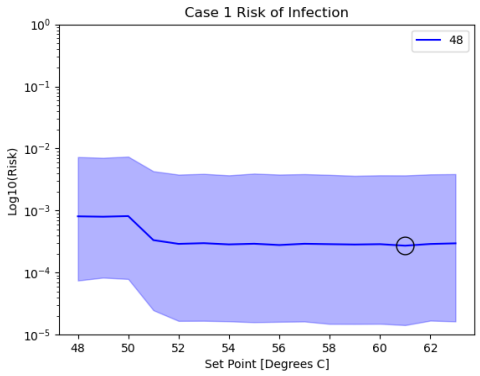	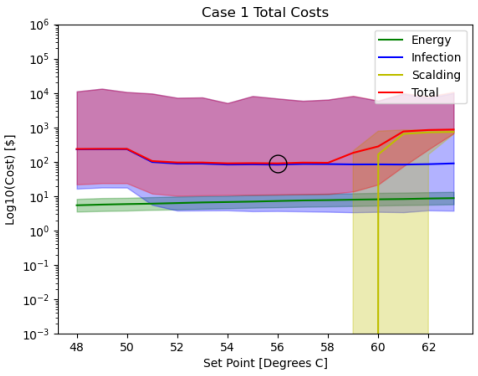
2	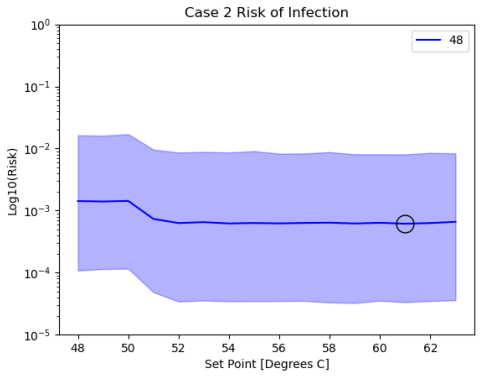	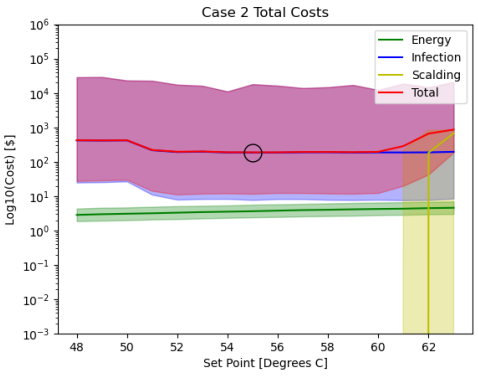
3	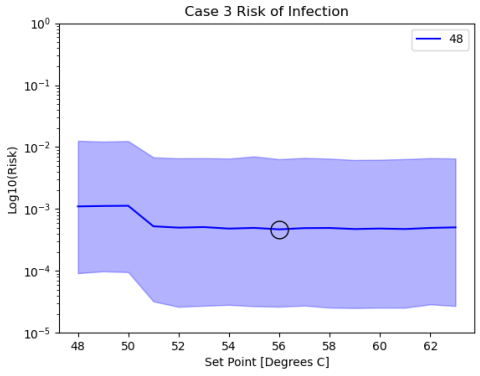	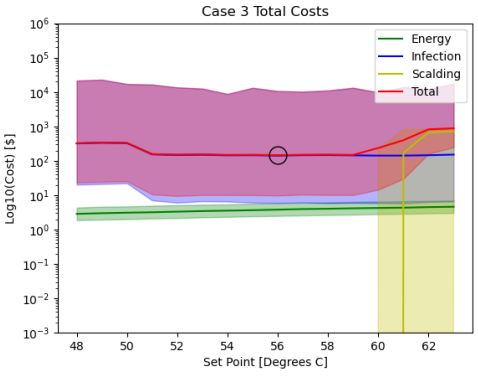

4	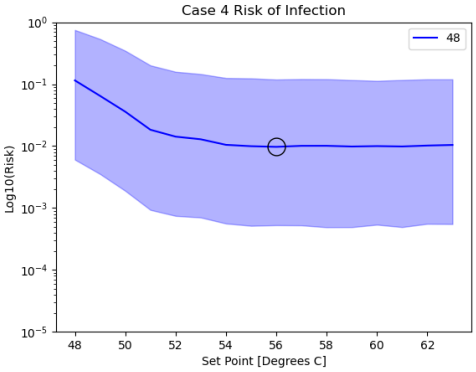 Case 4 Risk of Infection 48 Log10(Risk) Set Point [Degrees C]	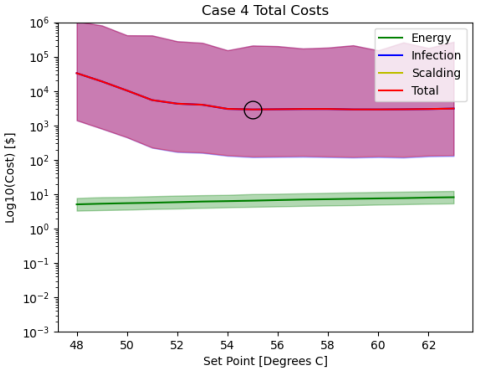 Case 4 Total Costs Energy Infection Scalding Total Log10(Cost) [$] Set Point [Degrees C]
5	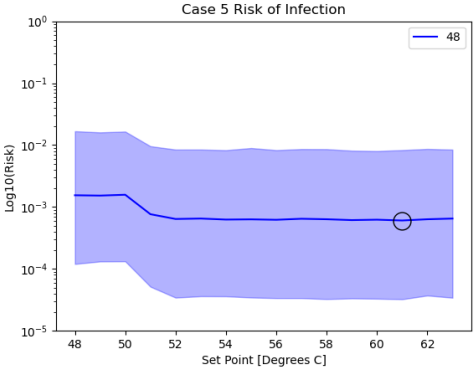 Case 5 Risk of Infection 48 Log10(Risk) Set Point [Degrees C]	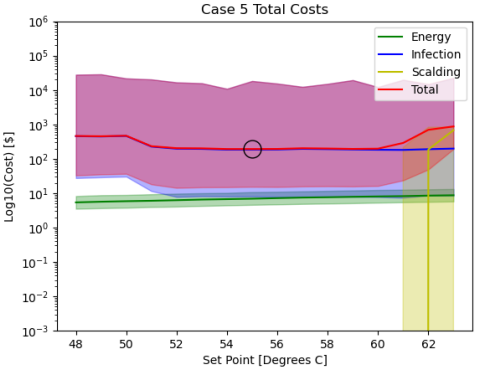 Case 5 Total Costs Energy Infection Scalding Total Log10(Cost) [$] Set Point [Degrees C]
6	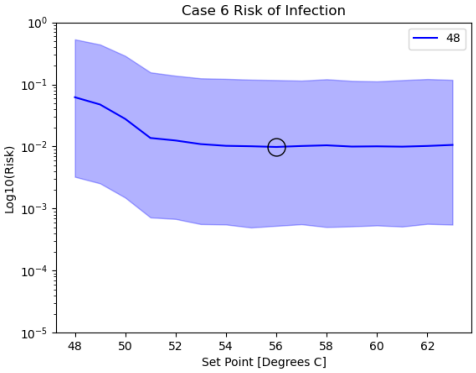 Case 6 Risk of Infection 48 Log10(Risk) Set Point [Degrees C]	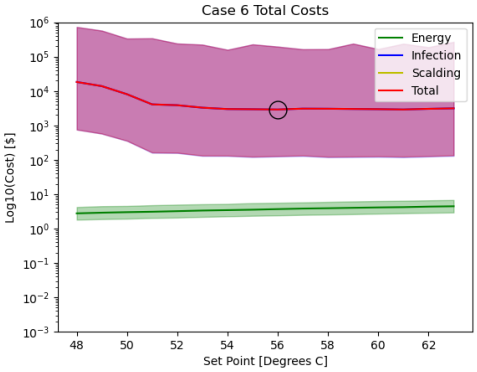 Case 6 Total Costs Energy Infection Scalding Total Log10(Cost) [$] Set Point [Degrees C]
7	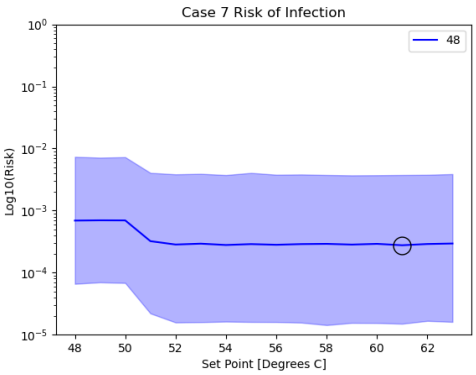 Case 7 Risk of Infection 48 Log10(Risk) Set Point [Degrees C]	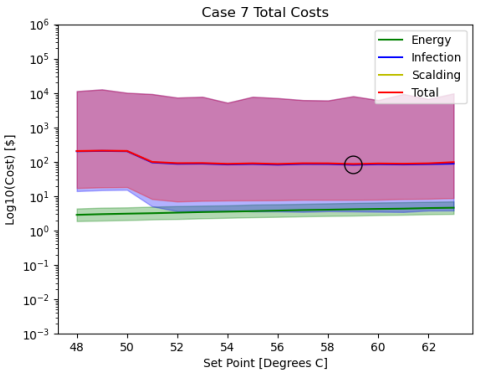 Case 7 Total Costs Energy Infection Scalding Total Log10(Cost) [$] Set Point [Degrees C]

8	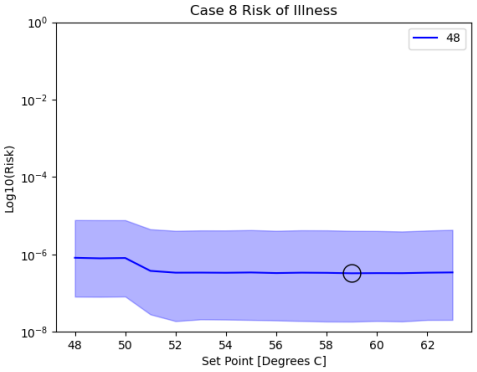 Case 8 Risk of Illness 48 Log10(Risk) Set Point [Degrees C]	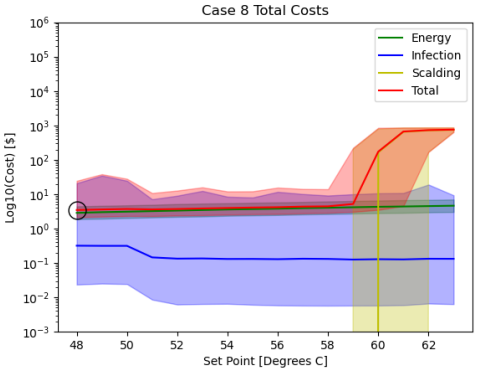 Case 8 Total Costs Energy Infection Scalding Total Log10(Cost) [$] Set Point [Degrees C]
9	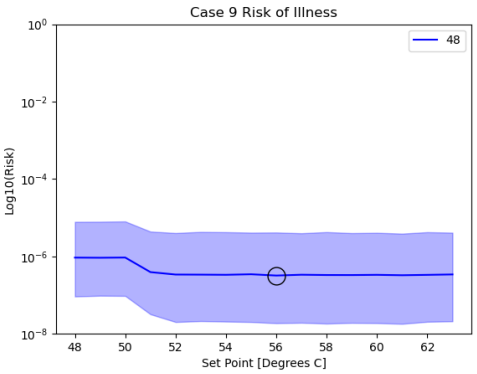 Case 9 Risk of Illness 48 Log10(Risk) Set Point [Degrees C]	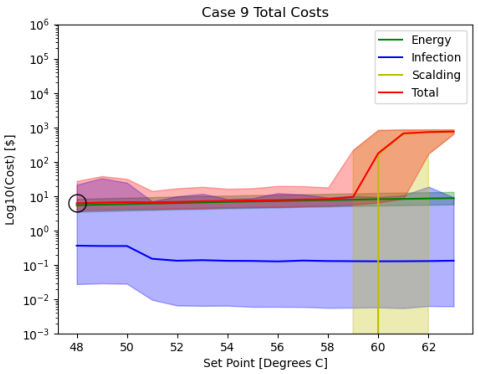 Case 9 Total Costs Energy Infection Scalding Total Log10(Cost) [$] Set Point [Degrees C]
10	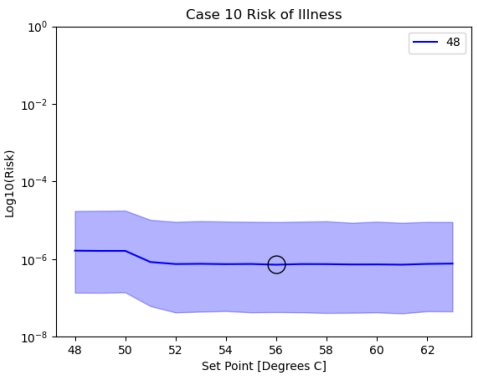 Case 10 Risk of Illness 48 Log10(Risk) Set Point [Degrees C]	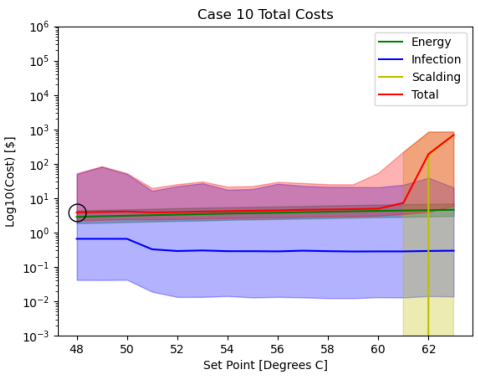 Case 10 Total Costs Energy Infection Scalding Total Log10(Cost) [$] Set Point [Degrees C]
11	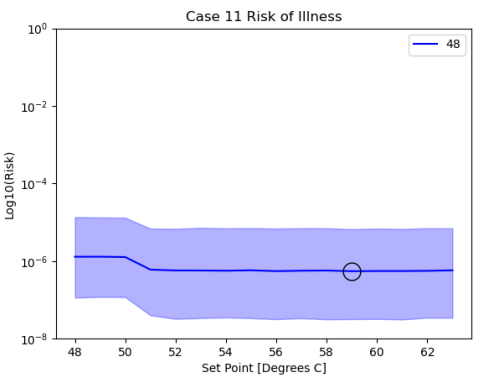 Case 11 Risk of Illness 48 Log10(Risk) Set Point [Degrees C]	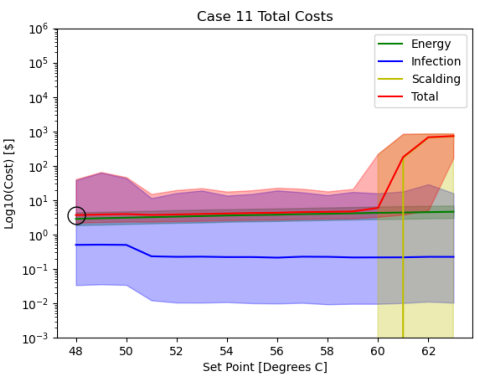 Case 11 Total Costs Energy Infection Scalding Total Log10(Cost) [$] Set Point [Degrees C]

12	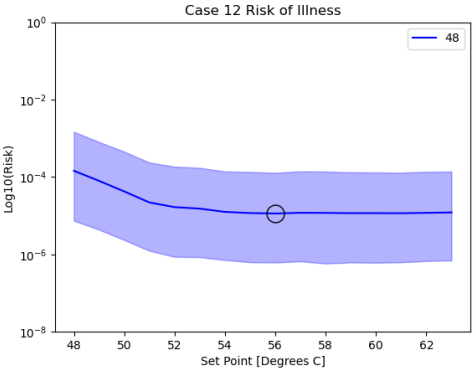 Case 12 Risk of Illness 48 Log10(Risk) Set Point [Degrees C]	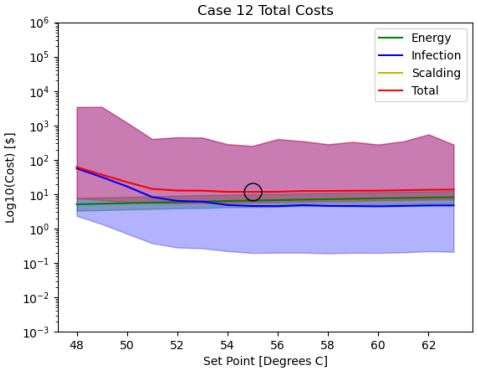 Case 12 Total Costs Energy Infection Scalding Total Log10(Cost) [$] Set Point [Degrees C]
13	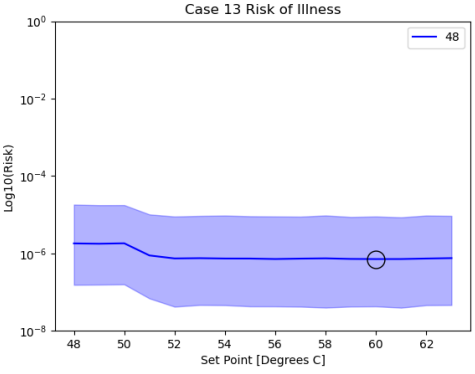 Case 13 Risk of Illness 48 Log10(Risk) Set Point [Degrees C]	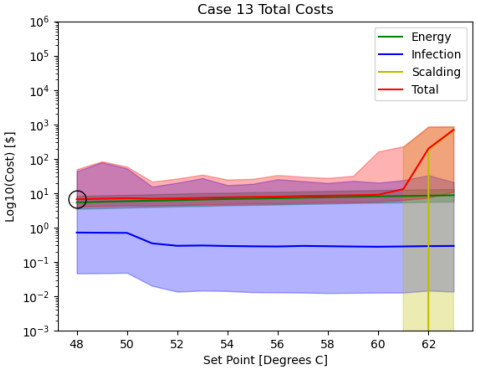 Case 13 Total Costs Energy Infection Scalding Total Log10(Cost) [$] Set Point [Degrees C]
14	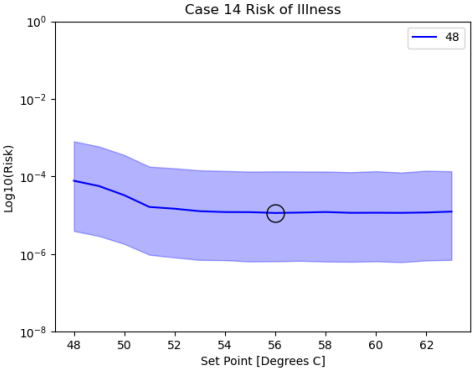 Case 14 Risk of Illness 48 Log10(Risk) Set Point [Degrees C]	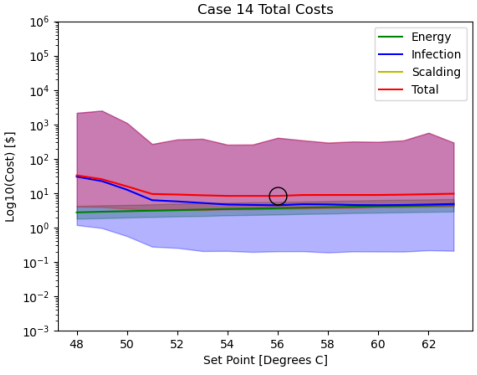 Case 14 Total Costs Energy Infection Scalding Total Log10(Cost) [$] Set Point [Degrees C]
15	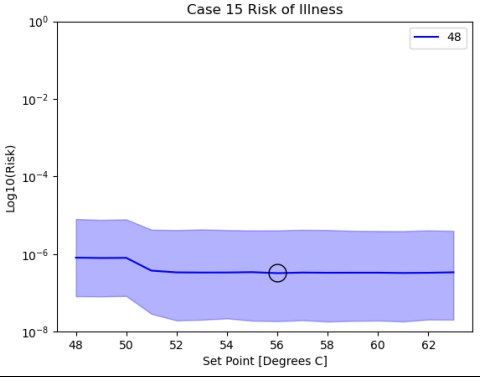 Case 15 Risk of Illness 48 Log10(Risk) Set Point [Degrees C]	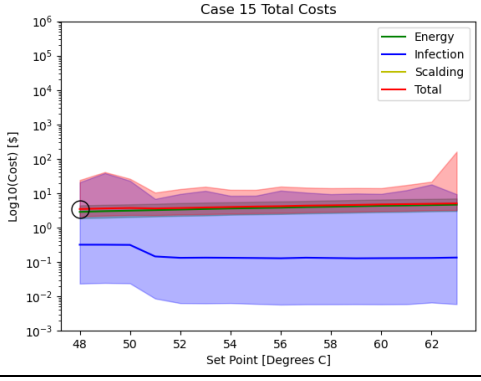 Case 15 Total Costs Energy Infection Scalding Total Log10(Cost) [$] Set Point [Degrees C]

Figure S14: Risk of illness or infection of Legionnaires Disease and total cost graphs for all cases.

References

1. Kleinbach EM, Beckman WA, Klein SA. Performance study of one-dimensional models for stratified thermal storage tanks. Solar Energy. 1993 Feb;50(2):155–66.

2. Westinghouse. Westinghouse Grid-Enabled Electric Water Heaters. 2020;2.

3. IAPMO. 2015 Minnesota Plumbing Code Water Pipe Sizing Workshop. IAPMO; 2016.

4. Blokker EJM, Pieterse-Quirijns EJ. Modeling temperature in the drinking water distribution system. Journal - American Water Works Association. 2013 Jan;105(1):E19–28.

5. Chmielewska A. Fluctuating temperature of the mains water throughout the year and its influence on the consumption of energy for the purposes of DHW preparation. Kaźmierczak B, Kutyłowska M, Piekarska K, Jadwiszczak P, editors. E3S Web Conf. 2018;44:00017.

6. Westinghouse. Westinghouse Grid-Enabled Electric Water Heater [Internet]. Westinghouse; 2017. Available from: http://www.westinghousewaterheating.com/literature/WEG-Brochure.pdf

7. EPA. Indoor Air Quality Tools for Schools Reference Guide [Internet]. EPA; 2009. Available from: https://www.epa.gov/sites/production/files/2014-08/documents/reference_guide.pdf

8. ASHRAE. ANSI/ASHRAE Standard 55: Thermal Environmental Conditions for Human Occupancy. ASHRAE [Internet]. 2010; Available from: http://arco-hvac.ir/wp-content/uploads/2015/11/ASHRAE-55-2010.pdf

9. AWWA. 2017 Water Utility Disinfection Survey Report [Internet]. American Water Works Association; 2018. Available from: https://www.awwa.org/Portals/0/AWWA/ETS/Resources/2017DisinfectionSurveyReport.pdf?ver=2018-12-21-163548-830

10. Borella P, Montagna MT, Romano-Spica V, Stampi S, Stancanelli G, Triassi M, et al. *Legionella* Infection Risk from Domestic Hot Water. Emerg Infect Dis. 2004 Mar;10(3):457–64.

11. Hamilton K, Hamilton MT, Johnson W, Jjemba P, Bukhari Z, LeChevallier M, et al. Risk-Based Critical Concentrations of *Legionella pneumophila* for Indoor Residential Water Uses. Environ Sci Technol. 2019 Apr 16;53(8):4528–41.

12. O'Toole J, Leder K, Sinclair M. A Series of Exposure Experiments−recycled Water and Alternative Water Sources. Part A. Aerosolsizing and Endotoxin Experiments. CRC for Water Quality and Treatment: Adelaide, Australia. 2008;

13. Incropera FP, Dewitt DP, Bergman TL, Lavine AS, editors. Fundamentals of heat and mass transfer. 6th ed. Hoboken, NJ: John Wiley; 2007. 997 p.

14. AWWARF. Characterization and Modeling of Chlorine Decay in Distribution Systems [Internet]. AWWA, USA; 1996. Available from: https://books.google.com/books?id=CG23TIEAuBUC&lpg=PR11&ots=v0ciIF6qnh&dq=AWWARF%20(1996)%20Characterisation%20and%20Modeling%20of%20Chlorine%20Decay%20in%20Distribution%20Systems.%20AWWA%2C%20USA.&lr&pg=PR11#v=onepage&q&f=false

15. Huang C, Shen Y, Smith RL, Dong S, Nguyen TH. Effect of disinfectant residuals on infection risks from Legionella pneumophila released by biofilms grown under simulated premise plumbing conditions. Environment International. 2020 Apr;137:105561.

16. Monteiro L, Figueiredo D, Dias S, Freitas R, Covas D, Menaia J, et al. Modeling of Chlorine Decay in Drinking Water Supply Systems Using EPANET MSX. Procedia Engineering. 2014;70:1192–200.

17. Sharaby Y, Rodríguez-Martínez S, Oks O, Pecellin M, Mizrahi H, Peretz A, et al. Temperature-Dependent Growth Modeling of Environmental and Clinical Legionella pneumophila Multilocus Variable-Number Tandem-Repeat Analysis (MLVA) Genotypes. Schaffner DW, editor. Appl Environ Microbiol. 2017 Apr 15;83(8):e03295-16, /aem/83/8/e03295-16.atom.

18. Yee RB, Wadowsky RM. Multiplication of Legionella pneumophila in Unsterilized Tap Water. APPL ENVIRON MICROBIOL. 1982;43:5.

19. Cervero-Aragó S, Rodríguez-Martínez S, Puertas-Bennasar A, Araujo RM. Effect of Common Drinking Water Disinfectants, Chlorine and Heat, on Free Legionella and Amoebae-Associated Legionella. Singer AC, editor. PLoS ONE. 2015 Aug 4;10(8):e0134726.

20. Kuchta JM, States SJ, McNamara AM, Wadowsky RM, Yee RB. Susceptibility of Legionella pneumophila to chlorine in tap water. Applied and Environmental Microbiology. 1983;46(5):1134–9.

21. Garny K, Neu TR, Horn H. Sloughing and limited substrate conditions trigger filamentous growth in heterotrophic biofilms—Measurements in flow-through tube reactor. Chemical Engineering Science. 2009 Jun;64(11):2723–32.

22. Thomas JM. The Risk to Human Health from Free-Living Amoebae Interaction with Legionella in Drinking and Recycled Water Systems. University of New South Wales; 2012.

23. Schoen ME, Ashbolt NJ. An in-premise model for Legionella exposure during showering events. Water Research. 2011 Nov;45(18):5826–36.

24. DeOreo WB, Mayer PW, Dziegielewski B, Kiefer J. Residential End Uses of Water, version 2. Water Research Foundation. 2016;18.

25. O'Toole J, Keywood M, Sinclair M, Leder K. Risk in the mist? Deriving data to quantify microbial health risks associated with aerosol generation by water-efficient devices during typical domestic water-using activities. Water Science and Technology. 2009 Dec 1;60(11):2913–20.

26. Allegra S, Leclerc L, Massard PA, Girardot F, Riffard S, Pourchez J. Characterization of aerosols containing Legionella generated upon nebulization. Sci Rep. 2016 Sep;6(1):33998.

27. Heyder J, Gebhart J, Rudolf G, Schiller C, Stahlhofen W. Deposition of particles in the human respiratory tract in the size range 0.005-15 micrometers. J Aerosol Sci. 1986;17(5):811–25.

28. Bussard D. U.S. EPA Exposure Factors Handbook 2011 Edition (Final Report). US Environmental Protection Agency, Washington, DC. 2011;EPA/600/R-09/052F:1436.

29. Armstrong TW, Haas CN. A Quantitative Microbial Risk Assessment Model for Legionnaires' Disease: Animal Model Selection and Dose-Response Modeling: A Quantitative Microbial Risk Assessment Model for Legionnaires' Disease. Risk Analysis. 2007 Dec 11;27(6):1581–96.

30. Muller D, Edwards ML, Smith DW. Changes in Iron and Transferrin Levels and Body Temperature in Experimental Airborne Legionellosis. The Journal of Infectious Diseases. 1983 Feb 1;147(2):302–7.

31. van Lier A, McDonald SA, Bouwknegt M, EPI group, Kretzschmar ME, Havelaar AH, et al. Disease Burden of 32 Infectious Diseases in the Netherlands, 2007-2011. Gregori L, editor. PLoS ONE. 2016 Apr 20;11(4):e0153106.

32. US Department of Health and Human Services. Guidelines for Regulatory Impact Analysis Appendix D: Updating Value per Statistical Life (VSL) Estimates for Inflation and Changes in Real Income [Internet]. ASPE. 2021 [cited 2021 Sep 14]. Available from: https://aspe.hhs.gov/reports/updating-vsl-estimates

33. Robinson LA, Hammitt JK. Valuing Reductions in Fatal Illness Risks: Implications of Recent Research: Valuing Reductions in Fatal Illness Risks. Health Econ. 2016 Aug;25(8):1039–52.

34. Weir MH, Mraz AL, Mitchell J. An Advanced Risk Modeling Method to Estimate Legionellosis Risks Within a Diverse Population. Water. 2019 Dec 20;12(1):43.

35. Moritz AR, Henriques FC. Studies of Thermal Injury: II. The Relative Importance of Time and Surface Temperature in the Causation of Cutaneous Burns. The American journal of pathology. 1947;23(5):695–720.

36. Blue Cross Blue Shield. Typical Costs for Common Medical Services. Blue Cross and Blue Shield of Massachusetts; 2009.

37. U.S. Energy Information Administration. Electric Power Monthly [Internet]. U.S. Energy Information Administration; Available from: https://www.eia.gov/electricity/monthly/epm_table_grapher.php?t=epmt_5_6_a

38. ENERGY STAR. ENERGY STAR Residential Water Heaters: Final Criteria Analysis [Internet]. ENERGY STAR; 2008. Available from: https://www.energystar.gov/ia/partners/prod_development/new_specs/downloads/water_heaters/waterheateranalysis_final.pdf